© 2014. Published by The Company of Biologists Ltd | Journal of Cell Science (2014) 127, 1052–1064 doi:10.1242/jcs.141226

RESEARCH ARTICLE

Podosomes of dendritic cells facilitate antigen sampling

Maksim V. Baranov*, Martin ter Beest*, Inge Reinieren-Beeren, Alessandra Cambi, Carl G. Figdor and Geert van den Bogaart‡

ABSTRACT

Dendritic cells sample the environment for antigens and play an important role in establishing the link between innate and acquired immunity. Dendritic cells contain mechanosensitive adhesive structures called podosomes that consist of an actin-rich core surrounded by integrins, adaptor proteins and actin network filaments. They facilitate cell migration via localized degradation of extracellular matrix. Here, we show that podosomes of human dendritic cells locate to spots of low physical resistance in the substrate (soft spots) where they can evolve into protrusive structures. Pathogen recognition receptors locate to these protrusive structures where they can trigger localized antigen uptake, processing and presentation to activate T-cells. Our data demonstrate a novel role in antigen sampling for the podosomes of dendritic cells.

KEY WORDS: Antigen presentation, Podosome, Dendritic cell, Receptor-mediated endocytosis

INTRODUCTION

The main function of dendritic cells is antigen presentation. Immature dendritic cells are localized in the spleen and other non-lymphoid tissues and constantly sample tissue and blood for antigens by so-called pattern recognition receptors (PRRs) (Lipscomb and Masten, 2002; McGreal et al., 2005; Takeda and Akira 2005; Kaparakis et al., 2007). Dendritic cells express many different PRRs that recognize pathogen-associated molecular patterns (PAMPs), such as lipopolysaccharide, from the outer membrane of gram-negative bacteria, as well as peptides of bacterial, fungal or viral origin. Binding of antigen to some PRRs, such as C-type lectins, can trigger uptake of antigen via receptor-mediated endocytosis or phagocytosis. Recognition of antigen results in maturation of dendritic cells and surface presentation of the antigen by major histocompatibility complex (MHC) molecules, upregulation of specific co-stimulatory molecules and finally migration to the lymph nodes, where dendritic cells prime T-cells (Banchereau and Steinman, 1998; McGreal et al., 2005). Because only dendritic cells can induce a primary immune response in resting naive T-lymphocytes, they are considered a crucial component that balances the innate and adaptive immune systems. For antigen sampling, immature dendritic cells need to migrate from their sites of origin (i.e. bone marrow) to specific sites of sampling activity (peripheral tissues), and for activation of T-cells, mature dendritic cells need to travel to the draining lymph nodes where they present antigen to T-cells.

Immature dendritic cells form particular cell–matrix contacts called podosomes that facilitate cell migration within peripheral tissues (reviewed in Buccione et al., 2004; Gimona et al., 2008; Linder et al., 2011; Murphy and Courtneidge, 2011; Schachtner et al., 2013b). Podosomes consist of an actin-rich core region surrounded by integrins from which anti-parallel actin filaments radiate (Schmidt et al., 2011; van den Dries et al., 2013b). Adaptor proteins such as vinculin, talin and paxillin connect the cortical actin cytoskeleton to the plasma membrane and to integrins, and are enriched around the actin-rich cores of podosomes. Unlike focal adhesions, podosomes contain the protein WASP that can recruit the actin nucleating complex Arp2/3 (Linder et al., 1999; Burns et al., 2001; Jones et al., 2002; Calle et al., 2006). Podosomes are points of concentrated release of the metalloproteinase MMP14 (also called MT1-MMP) and several other proteases that locally degrade the extracellular matrix (ECM) (van Helden et al., 2006; Gimona et al., 2008; Linder et al., 2011; Murphy and Courtneidge, 2011). Protease release at podosomes promotes cell invasiveness and facilitates cell migration through endothelium, epithelium and connective tissue (Matías-Román et al., 2005; Carman et al., 2007; Linder, 2007; Schachtner et al., 2013b). In fact, podosomes are commonly located at the leading edge of migrating cells and their turnover is required for cell migration and passage through endothelium (Burns et al., 2001; Calle et al., 2006). WASP-deficient leukocytes do not form podosomes and chemotactic migration is severely compromised in these cells (Zicha et al., 1998; Jones et al., 2002; Dovas et al., 2009). Podosomes are mechanosensitive (Collin et al., 2008) as demonstrated by their selective localization on the edges of 3D-micropatterned substrates (van den Dries et al., 2012).

Podosomes are not only formed by dendritic cells (Burns et al., 2001) but also by many other types of adherent cells, such as smooth muscle cells, endothelial cells, megakaryocytes, fibroblasts, macrophages, osteoclasts, microglia and at the postsynaptic site of the neuromuscular junction (Buccione et al., 2004; van Helden et al., 2006; Proszynski et al., 2009; Linder et al., 2011; Schachtner et al., 2013a). Although podosomes are very similar to the well-studied invadopodia of cancer cells (Wolf and Friedl, 2009), which are involved in cancer metastasis (Sabeh et al., 2004; Bravo-Cordero et al., 2012), they are considered to differ from invadopodia in at least two ways. First, podosomes are very dynamic with lifetimes that can be as short as 1 to 12 min, whereas invadopodia can persist

Department of Tumor Immunology, Radboud University Medical Centre, Radboud Institute for Molecular Life Sciences, Geert Grooteplein 28, 6525GA Nijmegen, The Netherlands.
*These authors contributed equally to this work.

‡Author for correspondence (mail@bogeert.com)

Received 21 August 2013; Accepted 9 December 2013

Journal of Cell Science

Journal of Cell Science (2014) 127, 1052–1064 doi:10.1242/jcs.141226

for hours (reviewed in Linder et al., 2011; Murphy and Courtneidge, 2011). Second, podosomes are smaller and measure only 0.5 to 2 µm in diameter and protrude only about 0.4 to 2 µm, whereas invadopodia can reach 8 µm in diameter and can protrude more than 5 µm from the cell surface into the extracellular environment (Linder et al., 2011; Murphy and Courtneidge, 2011). However, this limited protrusion depth of podosomes is contradicted in a recent study where it was shown that podosomes of dendritic cells could protrude more than 3 µm into the pores of polycarbonate filters (Gawden-Bone et al., 2010). Thus, the geometry of the substrate not only dictates the localization of podosomes (van den Dries et al., 2012), but might also affect the morphology of podosomes and allow podosomal protrusion into the extracellular environment.

The study by Gawden-Bone et al. (Gawden-Bone et al., 2010) demonstrated that when dendritic cells were cultured on filters, podosomes formed precisely on top of the pores and could extend into the lumen of the filter pores. Both the release of MMP14-containing vesicles and uptake of extracellular material occurred at the tips of these protrusive structures (Gawden-Bone et al., 2010). These results are interesting because dendritic cells are well known to be capable of sampling for antigen in the lumen of the lung, gut and small intestine by extending ‘protrusive dendrites’ through the epithelium of these organs (Rescigno et al., 2001; Niess et al., 2005; Chieppa et al., 2006; Vallon-Eberhard et al., 2006; Lelouard et al., 2012; Thornton et al., 2012; Farache et al., 2013; Shan et al., 2013; Strisciuglio et al., 2013). We speculated that this trans-epithelial antigen sampling might be related to the protrusive podosome-like structures first described by Gawden-Bone et al. (Gawden-Bone et al., 2010) and performed a molecular characterization of these actin-rich structures. Here, we demonstrate that podosomes of human dendritic cells can evolve into protrusive structures that help the cell to sample for antigen from deeper within the substrate. A wide range of PRRs locate to these protrusive structures where they can trigger receptor-mediated uptake of antigen. Our results show a direct role for podosomes in antigen presentation, and this constitutes a new mechanism of how cells might be able to sense extracellular signals through physical barriers.

RESULTS

Podosomes extend in soft spots of the substrate

When human dendritic cells are cultured on a glass substrate, they form clusters of podosomes (Fig. 1A) (Burns et al., 2001; van Helden et al., 2006). Podosomes on glass appear as dome-shaped actin-rich structures with an actin core of ~350 nm diameter and a height of ~500 nm, surrounded by a 250-nm wide ring of integrins and integrin-associated proteins, such as vinculin, talin

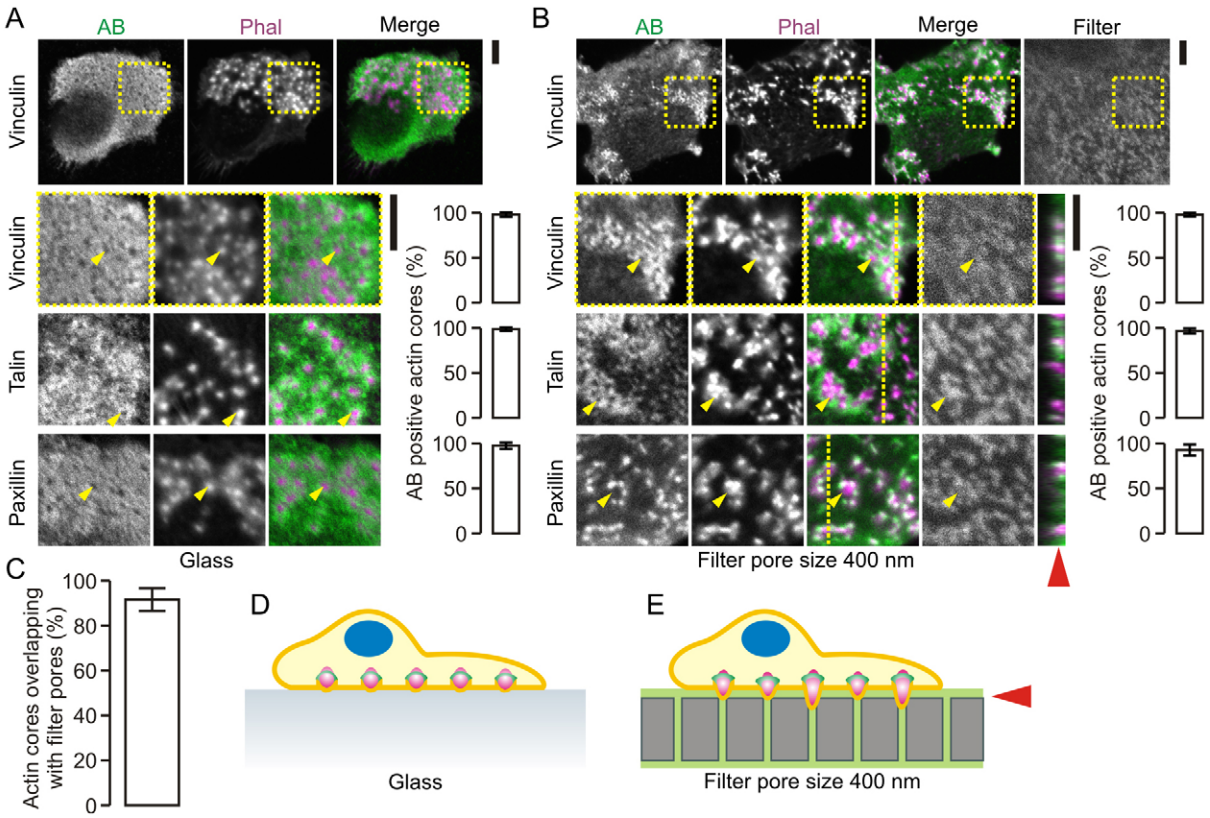

Fig. 1. Podosomes locate to spots of low physical resistance from the substrate. (A) Human-monocyte-derived dendritic cells cultured on glass substrate and stained with primary antibodies directed against vinculin, talin and paxillin, and secondary antibodies conjugated to Alexa Fluor 488 (AB, green). Actin was stained with phalloidin–Alexa-Fluor-564 (Phal, magenta). Shown are confocal images of representative cells with podosomes immediately at the glass surface. Yellow arrowheads indicate randomly chosen podosomes. Bar graphs show the percentage of AB-positive actin cores (means±s.d.). (B) Same as A, but cells were grown on polycarbonate filters with pore sizes of 400 nm. The filters were soaked in gelatin conjugated to Alexa Fluor 633 (Filter, gray). Yellow lines indicate the positions of the orthogonal views. The red arrowhead indicates the approximate location of the filter surface. (C) Quantification of the alignment of the podosomes to the filter pores from panel B (mean±s.d.). (D,E) Schemes of dendritic cells with non-protrusive podosomes on glass (D) and filters with pore sizes of 400 nm (E) (actin, magenta; vinculin, green). Scale bars: 5 µm.

Journal of Cell Science (2014) 127, 1052–1064 doi:10.1242/jcs.141226

and paxillin (Labernadie et al., 2010; Schmidt et al., 2011; Cox et al., 2011; van den Dries et al., 2012; van den Dries et al., 2013b). It has been recently reported that when dendritic cells are cultured on polycarbonate filters with pores of defined size, podosomes locate on top of the filter pores (Gawden-Bone et al., 2010). This alignment of the podosomes with the filter pores is likely related to the mechanosensitivity of podosomes that form around local deformations of the substrate (van den Dries et al., 2012). Indeed, when we cultured human dendritic cells for 1 hour on gelatin-soaked polycarbonate filters with 400-nm diameter pores, almost all podosomes formed directly on top of the filter pores (Fig. 1B–E). The actin-rich cores of these podosomes were surrounded by adaptor proteins, such as talin, vinculin and paxillin, similar to podosomes formed by cells on glass substrates (Linder et al., 2011). Optical *z*-sectioning by confocal microscopy revealed that these podosomes did not protrude into the lumen of the 400-nm-sized pores of the polycarbonate filters (less than 1 µm protrusion depth; Fig. 1B).

We speculated that a pore size of 400 nm might be too small to allow for protrusion of podosomes. To address this, we cultured dendritic cells on gelatin-impregnated filters with larger pores of 1 µm diameter, identical to those employed by Gawden-Bone et al. (Gawden-Bone et al., 2010). Indeed, as reported previously (Gawden-Bone et al., 2010), we observed clear protrusion of actin-rich structures into these 1-µm-sized pores (Fig. 2A) and regardless of whether the filters were impregnated with gelatin. The actin-rich core of these podosome-like structures could penetrate through the entire filter of ~10-µm thickness. The actin-rich cores were surrounded by adaptor proteins, such as vinculin, which was predominantly present at the base of the pores and did not seem to protrude into the 1-µm-sized pores. However, vinculin increasingly protruded into the lumen of the pores when cells were cultured on filters with larger pore sizes of 2 µm and 3 µm in diameter (Fig. 2B,C). On filters with these larger pore sizes, podosomes were not exclusively colocalized with the pores but were increasingly also present in between the pores (Fig. 2D). On filters with 3-µm-sized pores, small individual podosomes could be distinguished at the edges of the pores and the pore size was large enough to facilitate migration of the whole cell through the filter pores (Fig. 2C,E), as reported previously (Gawden-Bone et al., 2010). Thus, for cells cultured on polycarbonate filters with increasing pore sizes from 400 nm to 3 µm, the morphology of the podosomes differs; in smaller pores, the actin core and, in larger pores, adaptor proteins, such as vinculin, can progressively protrude into the lumen of the pores.

Overall, a picture is emerging where the initial non-protrusive podosomes of dendritic cells search for soft spots of low physical resistance in the substrate (e.g. the filter pores). When such a place is found, podosomes become increasingly invasive and can protrude into the substrate by local degradation of extracellular matrix and by exerting mechanical forces (Gawden-Bone et al., 2010; Labernadie et al., 2010). This results in growth of a protrusive podosome-like structure and at some point (i.e. for pores above 3 µm in diameter; Gawden-Bone et al., 2010) facilitates transmigration of the cell through physical barriers. Dendritic cells and other blood leukocytes have to cross blood vessel and lymphatic endothelium in order to activate the immune system (Muller, 2011; Vestweber, 2012). Secretion of the metalloproteinase MMP14 and turnover of podosomes are well-known to be essential for this transendothelium migration

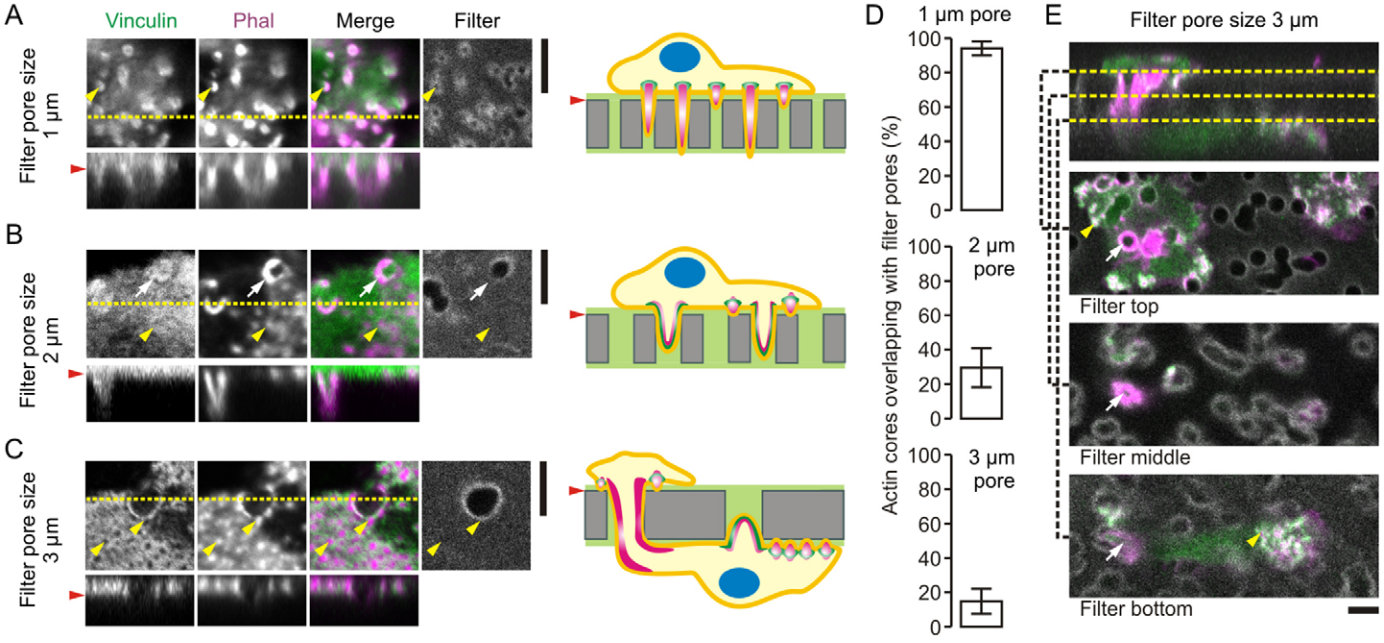

Fig. 2. Podosome-like protrusive structures of dendritic cells. (A) Dendritic cells cultured on polycarbonate membrane filters impregnated with Alexa-Fluor-633-labeled gelatin (gray) with pore sizes of 1 µm. Cells were immunostained for vinculin (green) and actin was visualized with phalloidin (Phal, magenta) similar to in Fig. 1. Shown are confocal sections just above the surface of the filters. The yellow line indicates the position of the orthogonal views showing the protrusion of actin in the lumen of the pores. Yellow arrowheads depict randomly selected actin-rich cores. The red arrowhead indicates the approximate filter surface. The right-hand panel shows a schematic diagram of the protrusions (actin: magenta; vinculin: green). (B) Same as A, but now for filters with pore sizes of 2 µm and showing the protrusion of both the actin core and vinculin in the pores as indicated by the white arrows. The cells also formed podosomes that did not overlap with the pores as indicated by the yellow arrowheads. (C) Same as B, but now with pore sizes of 3 µm. (D) Quantification of the fraction of actin cores aligning with the filter pores from panels A–C (means±s.d.). (E) Same as C, showing cell migration through the 3-µm pores in the filter (white arrows) and the formation of podosomes on both sides of the filter (yellow arrowheads). Confocal sections above, through and underneath the filter are shown. Scale bars: 5 µm.

Journal of Cell Science (2014) 127, 1052–1064 doi:10.1242/jcs.141226

(Matías-Román et al., 2005; Calle et al., 2006; Carman et al., 2007). Indeed, dendritic cells can migrate through monolayers formed by the endothelial cell line EA.hy926 (supplementary material Fig. S1A,B). Dendritic cells are also able to penetrate and pass monolayers formed by the epithelial cell line Caco-2 (supplementary material Fig. S1C–E) (Rescigno et al., 2001; Strisciuglio et al., 2013) and, for megakaryocytes, podosomes have also recently been shown to play a role in this epithelial penetration (Schachtner et al., 2013a). Thus, it is increasingly clear that podosomes facilitate cell migration across both endothelial and epithelial barriers.

Characterization of protrusive podosome-like structures

To further investigate the protrusive podosome-like structures on filter substrates, we performed immunostainings for typical podosomal marker proteins on dendritic cells cultured on filters with 1-µm pore sizes. Similar to podosomes of cells cultured on glass (Fig. 1A), the F-actin-rich core of protrusive podosome-like structures was surrounded by rings or clusters of talin, paxillin and the integrins ITGAM (a subunit of integrin αMβ2) and ITGB1 (integrin β1) (Fig. 3A). Interestingly, protrusive podosome-like structures often (for ~10–30% of all podosomes), but not always (for the remaining ~70–90% of podosomes), contained a ring of actin at the base of the protrusions, as could be observed with both phalloidin in fixed cells (Fig. 3B) and with the F-actin-binding probe LifeAct-GFP in live cells (supplementary material Fig. S2A,B). This is in clear contrast to podosomes formed by cells on glass substrate, which are generally considered to contain solid cores of actin (Fig. 1A). Integrins stimulate the production of phosphatidylinositol 4,5-bisphosphate (PIP_2), which stimulates WASP activity (Prehoda et al., 2000) and binds directly to talin and vinculin (Brakebusch and Fässler, 2003), and PIP_2 accumulates at and is essential for the formation of invadopodia of cancer cells (Yamaguchi et al., 2010). We therefore probed for PIP_2 by exogenously adding bacterially expressed pleckstrin homology domain of phospholipase C delta subunit fused to citrine (PLCδ-PH) (van den Bogaart et al., 2011). PLCδ-PH stained a ring surrounding the actin-rich core, demonstrating the presence of PIP_2

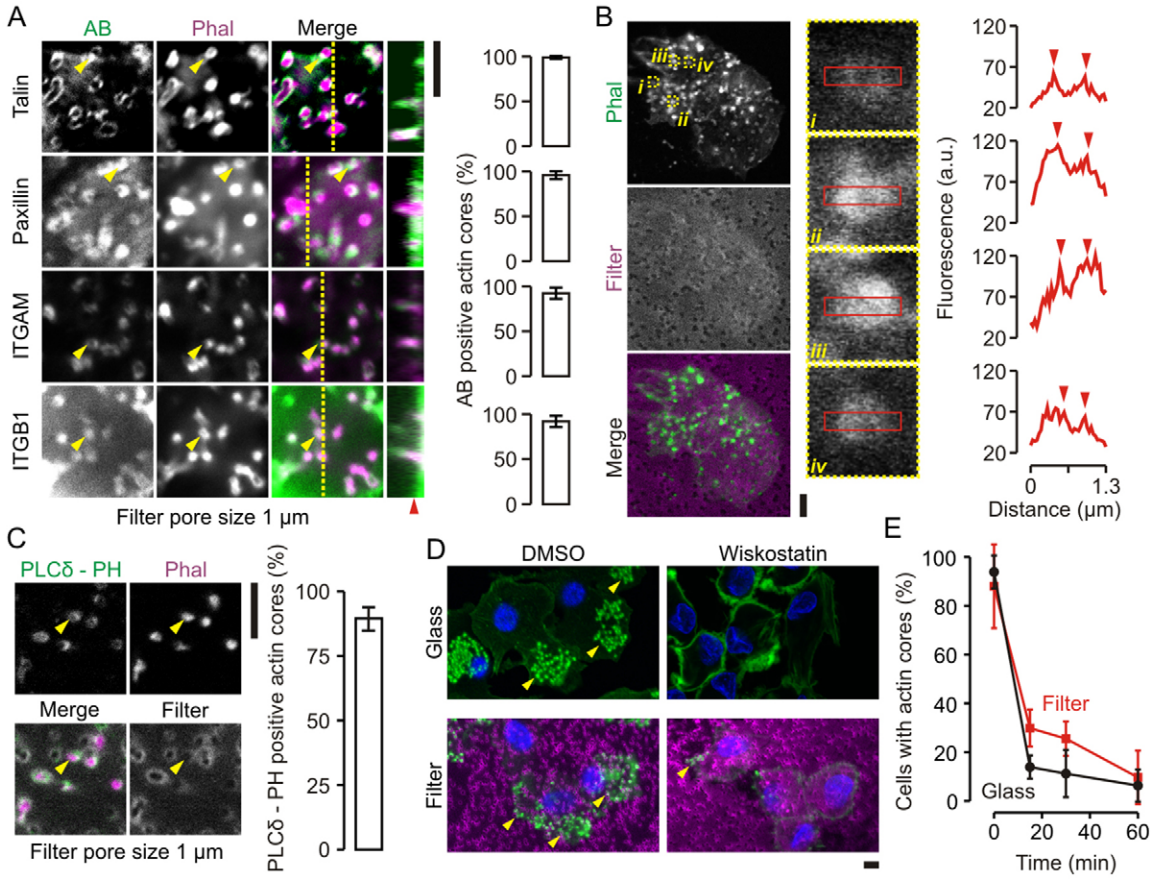

Fig. 3. Characterization of protrusive podosome-like structures. (A) Confocal images of human dendritic cells cultured on membrane filters with pore sizes of 1 µm. Actin was stained with phalloidin–Alexa-Fluor-546 (Phal, magenta) and talin, paxillin, ITGAM and ITGB1 were labeled by specific monoclonal antibodies and secondary antibodies conjugated to Alexa Fluor 488 (AB, green). Yellow lines indicate the positions of the orthogonal views. Yellow arrowheads indicate randomly chosen actin cores. The red arrowhead indicates the approximate surfaces of the filter substrates. Bar graphs show quantifications of the percentage of AB-positive actin cores (means±s.d.). (B) Confocal image of a dendritic cell on gelatin–Alexa-Fluor-633-impregnated filters with pore sizes of 1 µm (Filter, magenta) and stained with phalloidin–Alexa-Fluor-488 (green). The insets show magnifications of actin cores marked i–iv. The graphs show fluorescence intensity distributions through the cross-sections marked by the red boxes (*y*-averaging). The red arrowheads on the graph mark intensity peaks at the edges of the ring structures of some of the actin cores. (C) Staining of plasma membrane sheets of human dendritic cells similar to A, but instead of antibody staining, PIP_2 was labeled with bacterially expressed PLCδ-PH. (D) Cells precultured for 1 h on glass or gelatin–Alexa-Fluor-633-impregnated filters with pore sizes of 1 µm (magenta) were treated for 1 h with 5 µM of the WASP inhibitor wiskostatin or with carrier only (DMSO). Yellow arrowheads mark clusters of actin cores stained by phalloidin–Alexa-Fluor-488 (green). (E) The percentage of cells containing actin cores from the experiment described in D on glass (black) and filter (red) as a function of exposure time to wiskostatin (means±s.d., three independent repeats). Scale bars: 5 µm.

Journal of Cell Science (2014) 127, 1052–1064 doi:10.1242/jcs.141226

in this region (Fig. 3C). Podosome-like protrusive structures still depended on WASP (Linder et al., 1999; Burns et al., 2001; Jones et al., 2002; Calle et al., 2006), because treatment of the cells with wiskostatin, a selective and reversible inhibitor of WASP (Peterson et al., 2004), resulted in disassembly of the actin-rich protrusions at a similar rate to that of podosomes of cells cultured on glass (Fig. 3D,E) (Dovas et al., 2009; Tsujita et al., 2013).

Degradation of ECM occurs at podosomes and is dependent on the local release of metalloproteinases, such as MMP14 (Buccione et al., 2004; Gimona et al., 2008; Linder et al., 2011; Schachtner et al., 2013b). Indeed, degradation of ECM took place at protrusive podosome-like structures as apparent by the (~2-fold) local increased fluorescence intensity when the filters were impregnated with double-quenched FITC-labeled collagen in gelatin (Fig. 4A,B), in agreement with previous results (Gawden-Bone et al., 2010). We observed by immunocytochemistry that MMP14 was present in the protrusive podosome-like structures (formed on 1-µm-sized pores) and this is a clear difference from the (non-protrusive) podosomes of cells cultured on glass, where MMP14 was not enriched but rather seemed excluded from the actin-rich podosome cores (Wiesner et al., 2010) (Fig. 4C). MMP14-containing vesicles are known to traffic intracellularly on microtubules in a kinesin-mediated manner (Wiesner et al., 2010; Cornfine et al., 2011) and to travel via microtubules to the tip of invadopodia of cancer cells (Schoumacher et al., 2010). Our data suggest that MMP14-containing vesicles could also traffic via microtubules to the tip of protrusive podosome-like structures, because microtubules clearly penetrated the F-actin ring of these structures and extended into the lumen of the filter pores (Fig. 4D). This tubulin protrusion again is different from podosomes of cells cultured on glass, where the extension of the tubules into the podosomal cores was not observed.

The substrate influences the lifetime of podosomes, and periodic undulations of the actin-rich core are proposed to contribute to the protrusive and mechanosensitive properties of podosomes (Schachtner et al., 2013a; van den Dries et al., 2013a). Indeed, podosomes seem to become less dynamic and more stable when they become more invasive, because protrusive podosome-like structures have lifetimes that exceeded several hours compared to less than 1 h for podosomes on glass substrate. Moreover, the periodic undulations of the actin cores of protrusive podosome-like structures were reduced ~2-fold compared to podosomes of cells cultured on glass (supplementary material Fig. S2C–E; Movies 1, 2) (see also Labernadie et al., 2010; van den Dries et al., 2013a). Taken together, we conclude that when podosomes encounter spots of low physical resistance of the substrate (e.g. the filter pores), their morphology and protein composition change as they become increasingly more protrusive and less dynamic. We next addressed the role of endocytosis at these protrusive podosome-like structures of dendritic cells.

Protrusive podosome-like structures are involved in antigen sampling

In a previous study (Gawden-Bone et al., 2010), uptake of extracellular material at protrusive podosome-like structures of dendritic cells was shown by electron microscopy. In accordance with this observation, we found that the coat protein clathrin localized to these protrusive structures (Fig. 5A–C). Given that it is well-established that dendritic cells can sample for antigen across epithelial membranes (Rescigno et al., 2001; Niess et al., 2005; Chieppa et al., 2006; Vallon-Eberhard et al., 2006; Lelouard et al., 2012; Thornton et al., 2012; Farache et al., 2013; Shan et al., 2013; Strisciuglio et al., 2013) and as confirmed by our observations with monolayers of the epithelial cell line

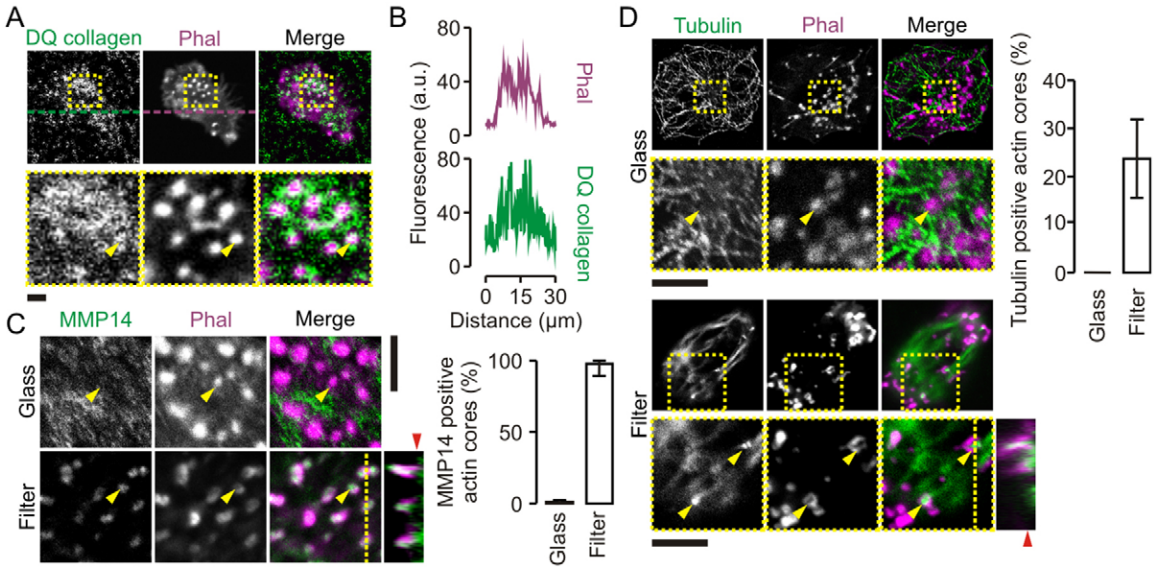

Fig. 4. Podosome-like protrusive structures contain MMP14 and tubulin. (A) Confocal images of dendritic cells cultured on filters with 1-µm pore size that were impregnated with double-quenched FITC-labeled collagen in gelatin (DQ collagen, green). Actin was stained with phalloidin–Alexa-Fluor-633 (Phal, magenta). Collagen degradation results in loss of self-quenching of the FITC fluorophore and an increase in fluorescence. (B) Fluorescence intensity profiles of the dashed lines marked in A. (C) Confocal images (left) and quantification (right) of dendritic cells cultured on glass and membrane filters with pore sizes of 1 µm. Actin was stained with phalloidin–Alexa-Fluor-546 (magenta), and the metalloproteinase MMP14 was labeled by specific monoclonal antibodies and secondary antibodies conjugated to Alexa Fluor 488 (AB, green). The yellow line indicates the positions of the orthogonal view. The yellow arrowheads indicate randomly chosen actin cores. The red arrowhead indicates the approximate surface of the filter. (D) Same as C, but for tubulin. Error bars show the spread of data for multiple cells from at least two independent experiments. Scale bars: 5 µm.

Journal of Cell Science (2014) 127, 1052–1064 doi:10.1242/jcs.141226

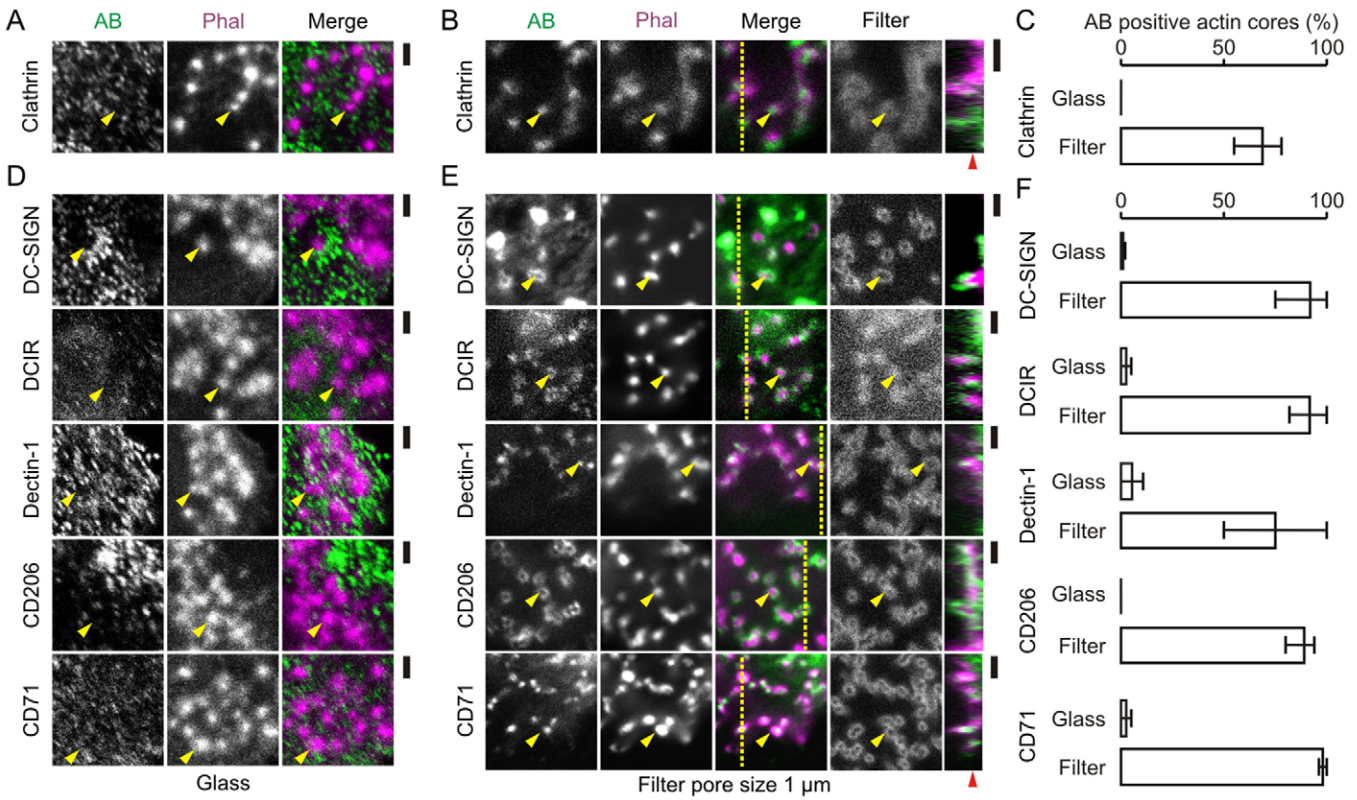

Fig. 5. Protrusive podosome-like structures contain pattern recognition receptors. (A,B) Confocal images of dendritic cells cultured on glass (A) and on filters with 1-µm pore size (B). Actin was labeled with phalloidin–Alexa-Fluor-546 (Phal, magenta) and clathrin was visualized by immunostaining (AB, green). The filters were impregnated with Alexa-Fluor-633-labeled gelatin (Filter, gray). The yellow line indicates the position of the orthogonal view. Yellow arrowheads indicate randomly selected actin-rich cores. The red arrowhead indicates the approximate filter surface. (C) Quantification of the percentage of clathrin-positive actin cores from the experiments described in A and B. (D–F) Same as A–C, but now with immunostaining for DC-SIGN, DCIR, Dectin-1, CD206 and CD71. Error bars show the spread of data for multiple cells from at least two independent experiments. Scale bars: 2 µm.

Caco-2 (supplementary material Fig. S1E), we hypothesized that antigen recognition and uptake might occur at the protrusive podosome-derived structures. In order to test this possibility, we first determined whether PRRs involved in antigen uptake located to these protrusive structures. We cultured monocyte-derived dendritic cells on filters with 1-µm pore sizes for 1 hour and performed immunostaining for various PRRs [the C-type lectin family receptors DC-SIGN (also known as CD209), DCIR (also known as CLEC4A), dectin-1 (also known as CLEC7A) and the mannose receptor CD206 (also known as MRC1)]. We also stained for the transferrin receptor CD71 (also known as TFRC) as a general endocytic receptor. All of these PRRs and CD71 localized to protrusive podosome-like structures, but not to non-protrusive podosomes on glass substrates (Fig. 5D–F). The presence of DC-SIGN and CD206 at these protrusive structures was confirmed by immunogold labeling followed by transmission electron microscopy (similar to Gawden-Bone et al., 2010), where we observed a ~3-fold (DC-SIGN) to ~9-fold (CD206) enrichment of gold beads at the protrusive structures compared to at the ventral membrane of the cells (i.e. membrane in contact with the filter surface) (Fig. 6). We subsequently determined the antigen sampling activity of these PRRs that localize to protrusive podosome-like structures.

We performed functional uptake experiments of quantum dots tethered to the HIV-1 envelope glycoprotein gp120 as a prototype antigen (Cambi et al., 2007); gp120 is a ligand for DC-SIGN (Geijtenbeek et al., 2000) and these gp120-coated quantum dots have a particle size of about 40 nm, which is comparable to the size of many viruses (Cambi et al., 2007). We also performed uptake experiments with OVA (ovalbumin), a well-characterized antigen and ligand for the mannose receptor CD206 (Burgdorf et al., 2006). Leakage experiments demonstrated that gelatin-impregnated filters were not or only poorly permeable to both OVA and gp120-quantum dots (Fig. 7A–C). We measured cellular uptake of gp120-quantum dots and of OVA through these gelatin-impregnated filters by fluorescence microscopy (Fig. 7D–F). Live-cell imaging showed that uptake of OVA through the filter occurred at the actin-rich protrusive structures (Fig. 7F). Uptake could be suppressed by the inhibitor of both clathrin-dependent (von Kleist et al., 2011) and independent (Dutta et al., 2012) endocytosis, Pitstop 2, indicating that uptake occurred via endocytosis (Fig. 7G).

Importantly, uptake of both gp120-quantum dots and OVA through the filters was promoted by the presence of protrusive podosome-like structures, because uptake was strongly reduced (1) when the dendritic cells were cultured on filters with a 400-nm pore size (where podosomes form but cannot protrude; Fig. 1B) (Fig. 8A,B) and (2) when CHO cells heterogeneously expressing recombinant DC-SIGN were used instead of dendritic cells (Fig. 8A). These CHO–DC-SIGN cells can take up gp120-quantum dots from the growth medium (Cambi et al., 2007), but do not form podosomes or podosome-like protrusions (supplementary material Fig. S3A). Moreover, uptake of OVA could be inhibited by the WASP inhibitor wiskostatin (Fig. 8C),

Journal of Cell Science (2014) 127, 1052–1064 doi:10.1242/jcs.141226

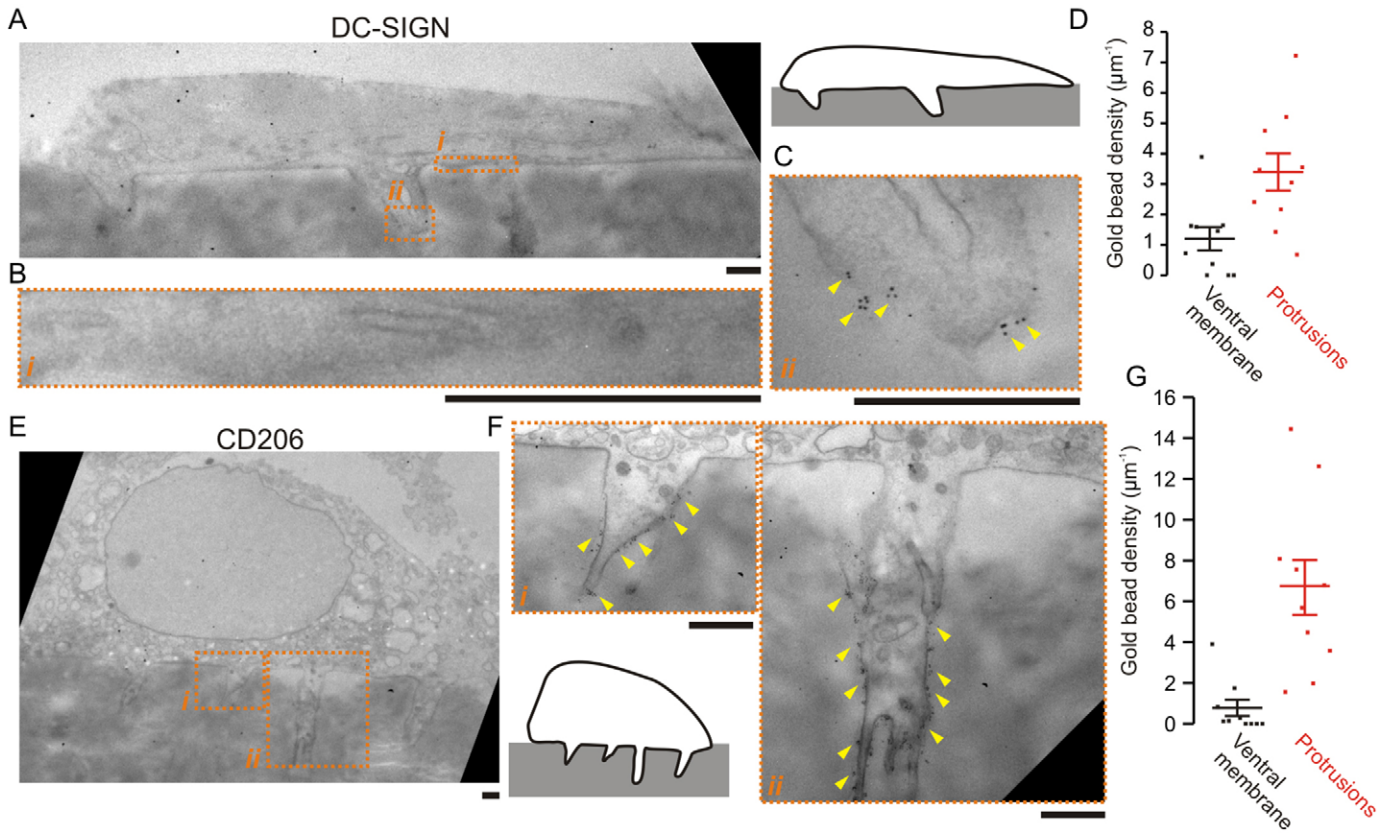

Fig. 6. Transmission electron microscopy of protrusive podosome-like structures. (A) Electron micrographs of a human dendritic cell cultured on a gelatin-impregnated filter with 1-μm pore size and immuno-gold labeled for DC-SIGN (an outline of the cell is shown to the upper-right of the micrograph). (B,C) Details of the ventral membrane (B, marked *i* in panel A) and of a protrusive structure (C, *ii*) from panel A. Yellow arrowheads mark positions of clusters of gold beads. (D) Quantification of the number of gold beads per μm in the ventral membrane (black) and the protrusions (red) for 10 different cells. Data points for individual cells and the means are shown (±s.e.m.). Bead density was increased 3-fold at the protrusions relative to ventral membrane (P=0.0005, two-tailed paired Student's t-test). (E) Same as A, but now with immuno-gold labeling for CD206, and the outline shown at the bottom right. (F) Magnifications of E as indicated (*i*, *ii*). (G) Same as D, but now for CD206. Bead density was increased 9-fold at the protrusions relative to ventral membrane (P=0.002, two-tailed paired Student's t-test). Scale bars: 1 μm.

which causes the disassembly of the protrusive structures (Fig. 3D,E). Although the rate of antigen uptake was decreased, uptake was not completely blocked in these control conditions, because of residual leakage of antigen through the filters and because the cells were still able to degrade gelatin. Uptake of gp120-quantum dots and OVA was antigen specific, because (1) uptake could be blocked by competitive inhibition with the sugar mannan (which binds to DC-SIGN and CD206) and (2) biotin-treated quantum dots (i.e. without gp120) were endocytosed substantially less effectively than gp120-quantum dots (Fig. 8A,B).

The antigen was not only taken up by the dendritic cells through the filters, but also subsequently processed by proteases, as apparent from the increase in fluorescence of double-quenched OVA (Fig. 8D,E). Degradation of this double-quenched OVA by proteases in endosomal/lysosomal compartments results in loss of fluorescent quenching and an increased fluorescence intensity. Control experiments with bafilomycin demonstrated that this processing was dependent on the acidification of endosomal/lysosomal compartments. Bafilomycin blocks the vesicular ATPase and thereby prevents the acidification required for activation of proteases. We performed experiments with dendritic cells isolated from mouse bone marrow (BMDCs) to determine whether dendritic cells that took up OVA antigen via podosomes could activate T-cells. Similar to human dendritic cells, these mouse BMDCs were able to form protrusive podosome-like structures on filters with 1-μm pore sizes and these protrusive structures contained vinculin, MMP14 and CD206 (the receptor for OVA antigen (Burgdorf et al., 2006) (supplementary material Fig. S3B). Finally, BMDCs that were loaded with OVA antigen via the filters could activate mouse hybridoma DO11.10 T-cells (supplementary material Fig. S3C). DO11.10 T-cells recognize OVA (323–339 epitope) bound to MHC class II and this results in an increased secretion of interleukin (IL)-2 (Shimonkevitz et al., 1983). However, owing to (1) the great sensitivity of T-cells, (2) the limited amount of dendritic cells we could culture on the filters (~10^3 cells) and (3) the inability to completely wash OVA from the gelatin coated filters (because of non-specific binding), we were unable to exclude the possibilities that antigen was directly taken up from the medium during the prolonged T-cell incubation step or that antigen leaked out of the cells or was regurgitated to be presented to the T-cells in trans rather than in cis. Nevertheless, colocalization experiments indicated that the antigen at least partly reached compartments containing MHC class II in human dendritic cells (Fig. 8F). We conclude that antigen uptake can occur at the protrusive structures of dendritic cells that contain podosomal elements and this antigen can be subsequently processed by dendritic cells, which might eventually result in T-cell activation.

Journal of Cell Science (2014) 127, 1052–1064 doi:10.1242/jcs.141226

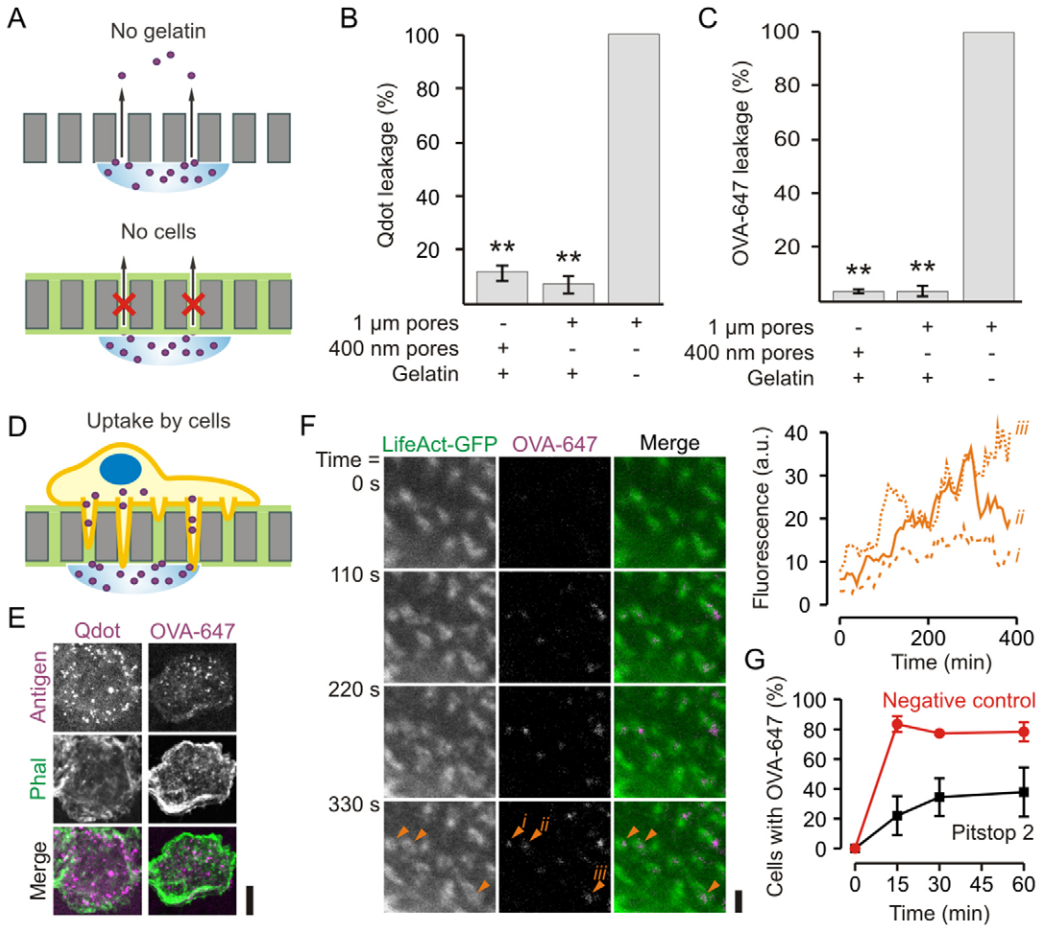

Fig. 7. Antigen uptake by protrusive podosome-like structures. (A) Schematics of the control experiments for passive leakage of quantum dots or OVA–Alexa-Fluor-647 (OVA-647) through the filters. (B,C) Leakage assay of quantum dots (B) or OVA-647 (C) through filters with different pore sizes and with or without gelatin impregnation. (D) Scheme of the antigen uptake experiments. (E) Confocal images of dendritic cells cultured on gelatin-coated filters with 1-µm pore sizes. A suspension of quantum dots linked to gp120 (Qdot; left, magenta) or a solution of OVA-647 (right, magenta) was applied to the other side of the filter. The cells were stained with phalloidin–Alexa-Fluor-488 (Phal, green) and imaged after 1 h incubation (see Fig. 8A,B for quantification). (F) Live-cell imaging of dendritic cells transfected with LifeAct-GFP and cultured on filter. At time $t=0$, OVA-647 was applied to the other side of the filter. The inset shows the increase of OVA-647 fluorescence in time at the position of the three actin cores marked with orange arrowheads (*i–iii*). The full dataset is in supplementary material Movie 3. (G) Time course of OVA-647 uptake for dendritic cells on filter treated with 20 µM Pitstop 2 (black) or Pitstop 2 negative control (red) (±s.e.m. of three independent repeats). Scale bars: 10 µm (E), 2 µm (F).

DISCUSSION

In this study, we demonstrate that podosomes can evolve into protrusive structures that can contribute to antigen sampling of dendritic cells. It is increasingly well established that podosomes respond to and sense the stiffness and geometry of the cellular substrate (Collin et al., 2008; Labernadie et al., 2010; van den Dries et al., 2012). Podosomes localize to spots of low physical resistance in the substrate. At these soft spots, podosomes exert physical forces (Labernadie et al., 2010) and locally degrade extracellular matrix through the concentrated release of metalloproteinases, such as MMP14 (Buccione et al., 2004; Gimona et al., 2008; West et al., 2008; Gawden-Bone et al., 2010; Linder et al., 2011; Schachtner et al., 2013b). This can result in remodeling of the ECM, and when or if pores are formed of sufficiently large size (>1 µm), podosomes become progressively protrusive and less dynamic and the morphology and protein composition of podosomes change. These findings are in agreement with the role of invasive podosome-like structures in the formation of transcellular pores in the endothelium (Carman et al., 2007).

At least at the base of protrusive podosome-like structures, actin forms a ring-shaped structure that aligns with the edges of the pore. This differs from (non-protrusive) podosomes on glass substrates, which are generally considered to consist of solid cores of actin, although recent stochastic optical reconstruction microscopy (STORM) super-resolution microscopy data from our group also seems to suggest in this case that there is an uneven distribution of actin in podosome cores that cannot be resolved by conventional diffraction-limited microscopy (van den Dries et al., 2013b). Microtubules penetrate the actin ring of the protrusive podosome-like structures and likely facilitate delivery of MMP14-containing vesicles to the protrusive tips (Wiesner et al., 2010; Cornfine et al., 2011), similar to in the invadopodia of cancer cells where this is well established (Schoumacher et al., 2010). This again differs from podosomes on glass substrates where MMP14-containing vesicles do not seem to reach the core but only transiently contact the periphery of podosomes (Wiesner et al., 2010) and, there, perhaps the dense actin cores prevent the entry of microtubules.

Journal of Cell Science (2014) 127, 1052–1064 doi:10.1242/jcs.141226

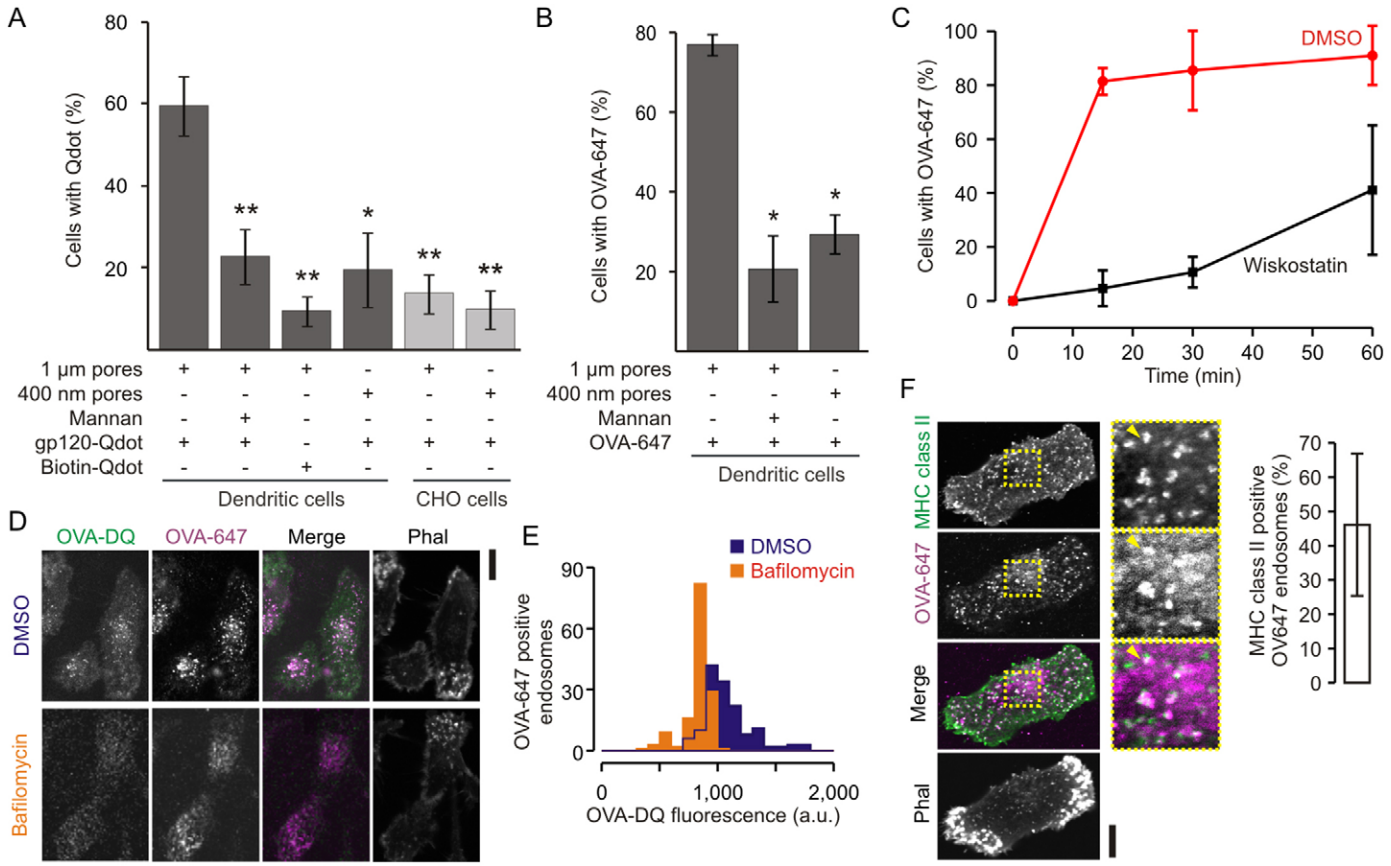

Fig. 8. Antigen uptake and processing by protrusive podosome-like structures. (A) Uptake assay as described in Fig. 7 for human dendritic cells and CHO cells stably expressing DC-SIGN cultured on gelatin-coated filters with 1-µm or 400-nm pore size and in the presence or absence of 25 µg ml^{-1} mannan. After 1 h of uptake, the percentage (±s.e.m.) of cells that took up gp120- or biotin-labeled quantum dots (gp120-Qdot and Biotin-Qdot, respectively) was determined by analysis of confocal images by two or three independent experts (>3 independent repeats; *P<0.02; **P<0.01). (B) Same as A, but now for OVA-647. (C) Time course of OVA-647 uptake for dendritic cells on filter treated with 5 µM wiskostatin (black) or carrier only (DMSO; red) (mean±s.e.m. of three independent repeats). (D) Confocal images of dendritic cells cultured on gelatin-coated filters with 1-µm pore size and with uptake of double-quenched OVA (OVA-DQ, green) and OVA–Alexa-Fluor-647 (OVA-647, magenta) through the filter. Actin was stained with phalloidin–Alexa-Fluor-564 (Phal, gray). OVA-DQ was dequenched, as apparent from the increased fluorescence compared to cells treated with bafilomycin A1. (E) Distribution of the OVA-DQ fluorescence of OVA-647-positive compartments for the bafilomycin-treated and control cells from the experiment shown in D (at least five cells each). (F) Uptake of OVA-647 (magenta) by dendritic cells on a filter, immunostained for MHC-class II (green). Actin was stained with phalloidin–Alexa-Fluor-546 (Phal, gray). Yellow arrowheads indicate intracellular compartments positive for MHC class II and OVA-647. The bar graphs show quantifications of compartments positive for MHC and OVA-647 (means±s.d.). Scale bars: 10 µm.

Eventually, the combined effects of the mechanical forces exerted by the podosomes and the protease-mediated degradation of extracellular material can allow for the complete cell to migrate through physical barriers. Here, pores in the substrate need to exceed a threshold size (~3 µm) (Gawden-Bone et al., 2010), which is likely limited by the size of the nucleus (Wolf et al., 2013). Migration of dendritic cells and other leukocytes through ECM and across endothelial membranes of blood and lymph vessels is crucial for immune system function (Muller, 2011; Vestweber, 2012), and our data further support the well-established role of podosomes in this process (Zicha et al., 1998; Burns et al., 2001; Jones et al., 2002; Matías-Román et al., 2005; Calle et al., 2006; Dovas et al., 2009).

In this study, we demonstrate a clear role of podosomes in antigen sampling of dendritic cells. We have shown that when podosomes become progressively protrusive, a variety of PRRs localize to these protrusive structures. These PRRs allow for receptor-mediated uptake of antigen from the protrusive tips (Gawden-Bone et al., 2010) and thereby can help the cell to sample for antigens from deeper within the substrate (i.e. from the other side of the polycarbonate filter). Antigen cannot only be taken up, but can also be subsequently processed and trafficked to MHC class II compartments and, after antigen presentation, this might result in T-cell activation. Interestingly, it has recently been reported that T-cells also employ protrusive podosome-like structures that contain T-cell receptors to probe for peptides presented in MHC (Sage et al., 2012), in clear analogy to our findings of antigen recognition by podosomes of dendritic cells.

A body of evidence suggests that dendritic cells can sample for antigen across lung, gut and small intestine epithelium (Rescigno et al., 2001; Niess et al., 2005; Chieppa et al., 2006; Vallon-Eberhard et al., 2006; Lelouard et al., 2012; Thornton et al., 2012; Farache et al., 2013; Shan et al., 2013; Strisciuglio et al., 2013). Here, dendritic cells can extend protrusive dendrites across the tight junctions of epithelial cells (Rescigno et al., 2001) or through transcellular pores in specialized microfold (M) cells (Lelouard et al., 2012); this facilitates the uptake of bacteria from the apical (lumen) side of the epithelial membrane. Our findings now suggest that these protrusive transepithelial dendrites might

have evolved from podosomes and thus could provide a mechanistic explanation for the capability of dendritic cells to phagocytose intra-epithelial bacteria.

In summary, we have shown that podosomes can sample the extracellular environment for spots of low mechanical resistance and, once such a spot is identified, podosomes can become increasingly protrusive. These protrusive structures not only facilitate cellular migration through extracellular matrix and endothelial membranes but can also be engaged in receptor-mediated uptake of antigen. Thereby podosomes can effectively increase the search area that a dendritic cell samples for antigen. This localized uptake of antigen from podosome-derived protrusive structures constitutes a novel role for podosomes of dendritic cells. Understanding how dendritic cells and other monocytes sample for antigen in the complex physical environment of the human body is crucial for our understanding of immune function.

MATERIALS AND METHODS

Preparation of human dendritic cells

Dendritic cells were derived from peripheral blood monocytes isolated from a buffy coat (de Vries et al., 2002). Monocytes isolated from healthy blood donors (informed consent obtained) were cultured for 6 days in RPMI 1640 medium (Life Technologies) containing 10% fetal bovine serum (FBS, Greiner Bio-one), 1 mM ultra-glutamine (BioWhittaker), antibiotics (100 U ml^{-1} penicillin, 100 µg ml^{-1} streptomycin and 0.25 µg ml^{-1} amphotericin B, Gibco), IL-4 (500 U ml^{-1}) and GM-CSF (800 U ml^{-1}) in a humidified, 5% CO_2-containing atmosphere.

Antibodies and reagents

The following primary antibodies were used for the immunofluorescence: mouse anti-vinculin (V9131, Sigma) at 1:200 dilution (v/v), mouse anti-talin (T3287, Sigma) at 1:100 (v/v), mouse anti-paxillin (349 | MAB3060, Sigma) at 1:100 (v/v), mouse anti-CD11b (ITGAM or Bear-1) (IM2581, Coulter) at 1:200 (v/v), mouse anti-CD29 (or ITGB1) (clone ts2/16) at 1:200 (v/v), mouse anti-MMP14 (MAB3328, Bio Connect/MilliPore) at 1:100 (v/v), rat anti-tubulin (ab6161, Abcam) at 1:500 (v/v), mouse anti-human CD209 (or DC-SIGN) (551186, BD Bioscience) at 1:200 (v/v), mouse anti-human DCIR (DDX0180, Dendritics) at 1:200 (v/v), mouse anti-human dectin-1 (MAB1859, R&D Systems) at 1:100 (v/v), mouse anti-human CD206 (555953, BD Biosciences) at 1:250 (v/v), mouse anti-human CD71 (347510, SALK) at 1:50 (v/v), mouse anti-clathrin light chain (C1985, Sigma) at 1:100 (v/v) and mouse anti-human MHC class II (clone Q5/13; Quaranta et al., 1980) at 20 µg ml^{-1}. The following secondary antibodies were used: goat anti-mouse IgG (H^+L) (A-11001), goat anti-rat IgG (H^+L) (A-11006) and goat anti-rabbit IgG (H^+L) (A-11008), all labeled with Alexa Fluor 488 dye (Invitrogen). Alexa-Fluor-488-, -546- and -633-conjugated phalloidin (Invitrogen) was used at dilutions of 1:200 (v/v) to stain F-actin. The quantum dot streptavidin conjugate (655 nm) was from Invitrogen (Q10121MP). Biotin rgp120 (HIV-1 III B) was purchased from ImmunoDiagnostics.

Gelatin impregnated filters

Gelatin was labeled with Alexa Fluor 633 by incubating 2% (w/v) gelatin from porcine skin in PBS with 100 µg ml^{-1} Alexa Fluor 633 succinimidyl ester (Invitrogen) for 30 min at room temperature. Unbound dye was removed by methanol precipitation of the gelatin. Hydrophilic polycarbonate membrane filters with different pore sizes (0.4, 1, 2 and 3 µm and 13 mm in diameter) (PCT0413100, PCT1025100, PCT2013100, PCT3013100; all from Sterlitech, Kent, WA) were washed first in 70% and then in 96% ethanol at room temperature. A 5-µl droplet of 2.5% gelatin in PBS was placed on top of a parafilm sheet (sterilized with ethanol) and a filter together with a coverslip was positioned on top of the gelatin solution. After 10 min of incubation, the filters were detached from the coverslips and subsequently transferred into a 24-well plate and kept in PBS until needed for cell culturing.

DQ-FITC-conjugated collagen (Invitrogen) was used for detection of ECM degradation. Human immature dendritic cells were grown for 1 h on filters prepared with 2.5 µg ml^{-1} DQ-collagen (type I from bovine skin conjugated with fluorescein) in 1% gelatin in PBS. Degraded collagen was visualized after fixation and staining for F-actin with phalloidin–Alexa-Fluor-633.

Immunofluorescence

Cells were cultured on filters at ~200,000 cells per filter (only several 1000 cells adhered) for 1 to 4 h and fixed for 15 min in 4% PFA in PBS at room temperature. Cells were then permeabilized with 0.1% (v/v) Triton X-100 in PBS for 5 min and blocked with CLSM-buffer [PBS with 20 mM glycine and 3% (w/v) BSA] for 30 min. For immunostaining, the cells were incubated with primary antibodies diluted in CLSM overnight at room temperature. Subsequently, the cells were washed with PBS and incubated with Alexa-Fluor-488-labeled secondary antibodies and Alexa-Fluor-546-conjugated phalloidin for 30 min. Finally, cells were washed with PBS prior to embedding in mounting medium containing 0.01% (v/v) Trolox (6-hydroxy-2,5,7,8-tetramethylchroman-2-carboxylic acid) and 68% (v/v) glycerol in 200 mM sodium phosphate buffer at pH 7.5. The cells were imaged with an Olympus FV1000 confocal laser scanning microscope (Olympus, Tokyo, Japan) with a 60× 1.35 NA oil immersion objective.

PIP_2 labeling

Human monocyte derived dendritic cells were grown on filters with 1 µm pores coated with 2.5% gelatin. Cells were disrupted by a brief ultrasound pulse as described previously (van den Bogaart et al., 2011) with some modifications. In brief, the filters with cells were washed twice with PBS at room temperature and placed on the bottom of a large glass container with PBS. The tip of the sonicator (Branson Digital Sonifier) was placed 3 cm above the filter and three pulses (10% power, 0.1 s pulse with 1 s interval) were given. Filters were then washed once with buffer containing 20 mM Hepes-KOH, 120 mM K-gluconate, 20 mM K-acetate, 2 mM ATP-Mg and 0.5 mM DTT, pH 7.4, and incubated for 30 min with 1 µM PLCδ-PH in the same buffer (van den Bogaart et al., 2011). Finally, the filters were washed twice with PBS, fixed with 4% PFA and co-stained with phalloidin–Alexa-Fluor-546.

Wiskostatin-mediated dissolution of podosomes

Dendritic cells were pre-cultured on glass or gelatin-impregnated filters for 1 h, followed by incubation for 15, 30, 60 and 120 min with 5 µM wiskostatin (40 mM stock in DMSO) and immediate fixation and immunostaining as described above.

OVA and gp120–quantum-dot uptake assay

For the conjugation of gp120 to quantum dots, 40 nM biotinylated gp120 was incubated with 20 nM quantum dots-655 with coupled avidin by mixing for 30 min at 4°C. The coupling was quenched by addition of a 10-fold molar excess of free biotin (to a final concentration of 200 nM) (Cambi et al., 2007).

To test the uptake of antigen via protrusive podosome-like structures, dendritic cells were pre-cultured for 2 h on filters with 1 µm and 400 nm pore sizes that were impregnated with gelatin. Then, the filters were inverted and placed on top of plastic rings filled with culture medium such that the medium contacted the cells on the filter. The opposite (upper) side of the filter was covered with 50 µl of a suspension of 1 nM quantum dots-655 conjugated to gp120. After a 30-minute incubation, the cells were fixed with 4% PFA and actin was stained with phalloidin–Alexa-Fluor-488. Cells were imaged by confocal microscopy. To test the uptake of OVA–Alexa-Fluor-647 antigen we performed the same assay as for gp120-quantum dots, but now we placed 50 µl of a 5 µg ml^{-1} OVA–Alexa-Fluor-647 on top of the filter.

Several control experiments were performed: (1) competitive inhibition of antigen uptake with 25 µg ml^{-1} mannan, (2) using quantum dots conjugated to biotin instead of gp120, (3) using filters with smaller pore sizes of 400 nm, (4) using CHO cells that stably expressed DC-SIGN (Cambi et al., 2007) instead of dendritic cells, and

(5) using wiskostatin and (6) Pitstop 2 block of antigen uptake. For the wiskostatin experiment, cells were preincubated for 30 min with 5 µM wiskostatin (40 mM stock in DMSO) and uptake experiments were performed in presence of wiskostatin. For the Pitstop 2 experiment, cells were preincubated for 15 min with 20 µM wiskostatin or the Pitstop 2 negative control (both from Abcam; 30 mM stock in DMSO) and uptake experiments were performed in presence of Pitstop 2 or negative control. All experiments were independently repeated at least three times with dendritic cells isolated from different donors and statistical significance (*P* values) was calculated with two-tailed Student's *t*-test for paired samples.

Passive leakage of antigen through gelatin-coated filters

In order to measure passive diffusion of the quantum dots and OVA through the filters we used either uncoated or gelatin-impregnated filters with pore sizes of 400 nm and 1 µm (prepared as described above). These filters were placed on top of plastic rings filled with PBS. A 50-µl droplet of antigen suspension (0.2 nM for gp120-labeled quantum dots and 5 µg ml^{-1} of OVA-647) was then placed on top of the filter for 30 min. The remaining volume of antigen suspension (~20 µl) was aspirated from the top of the filter and transferred to the MaxiSorp 96-well plate. The fluorescence intensity was measured with a CytoFluor ll fluorescence well plate reader (PerSeptive Biosystems) (quantum dots-655, excitation 360/40, emission 645/40 nm; OVA–Alexa-Fluor-647, excitation 590/20, emission 645/20 nm filters). Each experiment was repeated at least three times.

Live-cell imaging

Cells were transfected using the Neon Transfection system (Invitrogen) as described previously (van den Dries et al., 2013a). Briefly, ~200,000 cells were washed with PBS and resuspended in 100 µl resuspension buffer R (Invitrogen). These cells were subsequently mixed with 2 µg of a plasmid coding for LifeAct-GFP and electroporated (2 pulses of 40 ms, 1000 V). Transfected cells were plated in pre-warmed WillCo-dishes (WillCo Wells) containing antibiotic-free and serum-free RPMI medium (Invitrogen). After 3 h of culturing, the medium was replaced by medium supplemented with 10% (v/v) FCS and antibiotics. Prior to live cell imaging, cells were washed with PBS and imaging was performed in RPMI without Phenol Red supplemented with 10 mM HEPES at pH 7.4. Transiently transfected cells were imaged at 37℃ on a Zeiss LSM 510 microscope equipped with a PlanApochromatic 63× 1.4 NA oil immersion objective.

Transmission electron microscopy

For the immunogold labeling, dendritic cells were cultured on gelatin-impregnated filters with 1 µm pore size for 1 h, washed once with 0.1 M phosphate buffer at pH 7.4 (PB) and fixed with 2% (w/v) PFA in PB for 2 h. Residual PFA was quenched with 20 mM glycine in PB for 20 min. Samples were blocked with 5% (w/v) BSA-c and 0.1% (w/v) cold water fish gelatin in PB for 20 min. The sample was incubated with the primary antibody (directed against DC-SIGN or CD206) overnight at 4℃ in 0.1% BSA-c in PB, followed by incubation with secondary rabbit-anti-mouse antibody for 30 min at 20 µg ml^{-1}. For visualization, cells were incubated with protein A labeled with 10-nm-diameter gold particles (binds rabbit IgG) in 0.1% BSA-c in PB. A final fixation step was performed with 2% glutaraldehyde in PB for 60 min at 4℃. Samples were treated for 60 min with 1% (w/v) OsO_4, 1% (w/v) potassium ferrocyanide in 0.1 M sodium cacodylate buffer at pH 7.4. Following dehydration with a graded ethanol series, the filters were embedded in Epon which was left to polymerize for 24 h at 60℃. After polymerization, ~90-nm thin sections perpendicular to the surface of the filter surfaces were cut with a microtome and specimens were imaged with a JEOL 1010 transmission electron microscope.

Transwell inserts with endothelial and epithelial monolayers

Costar Transwell 6.5-mm diameter inserts containing polycarbonate membrane filters with a 5-µm pore size (catalogue number 3421; Corning Incorporated) and impregnated with gelatin were cultured with ~160,000 cells of the endothelial cell line EA.hy926 in DMEM with 4.5 g l^{-1} glucose, 1 mM ultra-glutamine, antibiotics and 10% FBS on the outer side of the inserts. For the epithelial cell line Caco-2, ~5000 cells were cultured in DMEM with 25 mM glucose, 1% non-essential amino acids, antibiotics and 20% FBS on the outer side of the inserts and without gelatin. Confluent monolayers were formed after 10 days (for EA.hy926) and 20 days (for Caco-2) culturing time. Subsequently, ~20,000 to 100,000 dendritic cells were applied to the inner chamber of the transwell inserts and incubated for 24 h (for EA.hy926) or 5 h (for Caco-2). For the uptake experiments of Alexa-Fluor-647-labeled ovalbumin (OVA-647) through the monolayers of Caco-2 cells (supplementary material Fig. S1E), 5 µg ml^{-1} OVA-647 in RPMI was added to the outer chamber and incubated for 1 h. Finally, the samples were fixed and immunostained for DC-SIGN and CD206 (expressed by dendritic cells).

ELISA and DO11.10 activation assay

For measuring IL-2 production, as a readout of T-cell activation, we used the T-cell hybridoma line DO11.10. DO11.10 cells were grown in IMDM with 5% FCS, 1 mM ultra-glutamine, antibiotics and 0.1% (v/v) β-mercaptoethanol. Immature mouse bone-marrow-derived dendritic cells (BMDCs) were isolated by culturing for 7 days with GM-CSF (20 ng ml^{-1}). Animal studies were approved by the Animal Ethics Committee of the Nijmegen Animal Experiments Committee. The OVA antigen (concentration used 100 µg ml^{-1}) uptake assay on filters (1 µm pores) was performed as described above for 1 h. The filters were washed three times with PBS, and DO11.10 cells in RPMI were added to the washed filters and incubated overnight. ~200,000 BMDCs and 1×10^6 DO11.10 cells were used, but the ratio of BMDC to T-cells was in the order of 1:20–1:200 given that only a fraction of the BMDCs adhered to the filter (1000–10,000 cells). After culturing for 6 days, IL-2 production was measured by using monoclonal capture and HRP-conjugated anti-IL-2 antibodies (554424 and 554426, BD Biosciences) using standard ELISA procedures.

Acknowledgements

We thank Peter Friedl for comments, Jack Fransen for Caco-2 cells and Mietske Wijers for help with the electron microscopy (all Radboud University Medical Centre, The Netherlands).

Competing interests

The authors declare no competing interests.

Author contributions

M.V.B., M.t.B. and G.v.d.B. designed and performed the experiments and wrote the paper. I.R.B. assisted in the electron microscopy. M.V.B., M.t.B., G.v.d.B., A.C. and C.G.F. discussed the results and commented on the manuscript.

Funding

G.v.d.B. is funded by a fellowship from the Radboud University Medical Centre and is the recipient of a Starting Grant from the European Research Council under the European Union's Seventh Framework Programme [grant agreement number 336479]. A.C. is the recipient of a grant of the Human Frontier Science Program Organization and of a Meervoud grant from the Netherlands Organization for Scientific Research (NWO). C.G.F. is the recipient of an Advanced Grant from the European Research Council under the European Union's Seventh Framework Programme and of a Spinoza award from NWO. Deposited in PMC for immediate release.

Supplementary material

Supplementary material available online at
http://jcs.biologists.org/lookup/suppl/doi:10.1242/jcs.141226/-/DC1

References

Banchereau, J. and Steinman, R. M. (1998). Dendritic cells and the control of immunity. *Nature* **392**, 245-252.
Brakebusch, C. and Fässler, R. (2003). The integrin-actin connection, an eternal love affair. *EMBO J.* **22**, 2324-2333.
Bravo-Cordero, J. J., Hodgson, L. and Condeelis, J. (2012). Directed cell invasion and migration during metastasis. *Curr. Opin. Cell Biol.* **24**, 277-283.
Buccione, R., Orth, J. D. and McNiven, M. A. (2004). Foot and mouth: podosomes, invadopodia and circular dorsal ruffles. *Nat. Rev. Mol. Cell Biol.* **5**, 647-657.

Burgdorf, S., Lukacs-Kornek, V. and Kurts, C. (2006). The mannose receptor mediates uptake of soluble but not of cell-associated antigen for cross-presentation. *J. Immunol.* **176**, 6770-6776.
Burns, S., Thrasher, A. J., Blundell, M. P., Machesky, L. and Jones, G. E. (2001). Configuration of human dendritic cell cytoskeleton by Rho GTPases, the WAS protein, and differentiation. *Blood* **98**, 1142-1149.
Calle, Y., Carragher, N. O., Thrasher, A. J. and Jones, G. E. (2006). Inhibition of calpain stabilises podosomes and impairs dendritic cell motility. *J. Cell Sci.* **119**, 2375-2385.
Cambi, A., Lidke, D. S., Arndt-Jovin, D. J., Figdor, C. G. and Jovin, T. M. (2007). Ligand-conjugated quantum dots monitor antigen uptake and processing by dendritic cells. *Nano Lett.* **7**, 970-977.
Carman, C. V., Sage, P. T., Sciuto, T. E., de la Fuente, M. A., Geha, R. S., Ochs, H. D., Dvorak, H. F., Dvorak, A. M. and Springer, T. A. (2007). Transcellular diapedesis is initiated by invasive podosomes. *Immunity* **26**, 784-797.
Chieppa, M., Rescigno, M., Huang, A. Y. and Germain, R. N. (2006). Dynamic imaging of dendritic cell extension into the small bowel lumen in response to epithelial cell TLR engagement. *J. Exp. Med.* **203**, 2841-2852.
Collin, O., Na, S., Chowdhury, F., Hong, M., Shin, M. E., Wang, F. and Wang, N. (2008). Self-organized podosomes are dynamic mechanosensors. *Curr. Biol.* **18**, 1288-1294.
Cornfine, S., Himmel, M., Kopp, P., El Azzouzi, K., Wiesner, C., Krüger, M., Rudel, T. and Linder, S. (2011). The kinesin KIF9 and reggie/flotillin proteins regulate matrix degradation by macrophage podosomes. *Mol. Biol. Cell* **22**, 202-215.
Cox, S., Rosten, E., Monypenny, J., Jovanovic-Talisman, T., Burnette, D. T., Lippincott-Schwartz, J., Jones, G. E. and Heintzmann, R. (2011). Bayesian localization microscopy reveals nanoscale podosome dynamics. *Nat. Methods* **9**, 195-200.
de Vries, I. J., Eggert, A. A., Scharenborg, N. M., Vissers, J. L., Lesterhuis, W. J., Boerman, O. C., Punt, C. J., Adema, G. J. and Figdor, C. G. (2002). Phenotypical and functional characterization of clinical grade dendritic cells. *J. Immunother.* **25**, 429-438.
Dovas, A., Gevrey, J. C., Grossi, A., Park, H., Abou-Kheir, W. and Cox, D. (2009). Regulation of podosome dynamics by WASp phosphorylation: implication in matrix degradation and chemotaxis in macrophages. *J. Cell Sci.* **122**, 3873-3882.
Dutta, D., Williamson, C. D., Cole, N. B. and Donaldson, J. G. (2012). Pitstop 2 is a potent inhibitor of clathrin-independent endocytosis. *PLoS ONE* **7**, e45799.
Farache, J., Koren, I., Milo, I., Gurevich, I., Kim, K. W., Zigmond, E., Furtado, G. C., Lira, S. A. and Shakhar, G. (2013). Luminal bacteria recruit CD103+ dendritic cells into the intestinal epithelium to sample bacterial antigens for presentation. *Immunity* **38**, 581-595.
Gawden-Bone, C., Zhou, Z., King, E., Prescott, A., Watts, C. and Lucocq, J. (2010). Dendritic cell podosomes are protrusive and invade the extracellular matrix using metalloproteinase MMP-14. *J. Cell Sci.* **123**, 1427-1437.
Geijtenbeek, T. B., Kwon, D. S., Torensma, R., van Vliet, S. J., van Duijnhoven, G. C., Middel, J., Cornelissen, I. L., Nottet, H. S., KewalRamani, V. N., Littman, D. R. et al. (2000). DC-SIGN, a dendritic cell-specific HIV-1-binding protein that enhances trans-infection of T cells. *Cell* **100**, 587-597.
Gimona, M., Buccione, R., Courtneidge, S. A. and Linder, S. (2008). Assembly and biological role of podosomes and invadopodia. *Curr. Opin. Cell Biol.* **20**, 235-241.
Jones, G. E., Zicha, D., Dunn, G. A., Blundell, M. and Thrasher, A. (2002). Restoration of podosomes and chemotaxis in Wiskott-Aldrich syndrome macrophages following induced expression of WASp. *Int. J. Biochem. Cell Biol.* **34**, 806-815.
Kaparakis, M., Philpott, D. J. and Ferrero, R. L. (2007). Mammalian NLR proteins; discriminating foe from friend. *Immunol. Cell Biol.* **85**, 495-502.
Labernadie, A., Thibault, C., Vieu, C., Maridonneau-Parini, I. and Charrière, G. M. (2010). Dynamics of podosome stiffness revealed by atomic force microscopy. *Proc. Natl. Acad. Sci. USA* **107**, 21016-21021.
Lelouard, H., Fallet, M., de Bovis, B., Méresse, S. and Gorvel, J. P. (2012). Peyer's patch dendritic cells sample antigens by extending dendrites through M cell-specific transcellular pores. *Gastroenterology* **142**, 592-601, e3.
Linder, S. (2007). The matrix corroded: podosomes and invadopodia in extracellular matrix degradation. *Trends Cell Biol.* **17**, 107-117.
Linder, S., Nelson, D., Weiss, M. and Aepfelbacher, M. (1999). Wiskott-Aldrich syndrome protein regulates podosomes in primary human macrophages. *Proc. Natl. Acad. Sci. USA* **96**, 9648-9653.
Linder, S., Wiesner, C. and Himmel, M. (2011). Degrading devices: invadosomes in proteolytic cell invasion. *Annu. Rev. Cell Dev. Biol.* **27**, 185-211.
Lipscomb, M. F. and Masten, B. J. (2002). Dendritic cells: immune regulators in health and disease. *Physiol. Rev.* **82**, 97-130.
Matías-Román, S., Gálvez, B. G., Genís, L., Yáñez-Mó, M., de la Rosa, G., Sánchez-Mateos, P., Sánchez-Madrid, F. and Arroyo, A. G. (2005). Membrane type 1-matrix metalloproteinase is involved in migration of human monocytes and is regulated through their interaction with fibronectin or endothelium. *Blood* **105**, 3956-3964.
McGreal, E. P., Miller, J. L. and Gordon, S. (2005). Ligand recognition by antigen-presenting cell C-type lectin receptors. *Curr. Opin. Immunol.* **17**, 18-24.
Muller, W. A. (2011). Mechanisms of leukocyte transendothelial migration. *Annu. Rev. Pathol.* **6**, 323-344.
Murphy, D. A. and Courtneidge, S. A. (2011). The 'ins' and 'outs' of podosomes and invadopodia: characteristics, formation and function. *Nat. Rev. Mol. Cell Biol.* **12**, 413-426.
Niess, J. H., Brand, S., Gu, X., Landsman, L., Jung, S., McCormick, B. A., Vyas, J. M., Boes, M., Ploegh, H. L., Fox, J. G. et al. (2005). CX3CR1-mediated dendritic cell access to the intestinal lumen and bacterial clearance. *Science* **307**, 254-258.
Peterson, J. R., Bickford, L. C., Morgan, D., Kim, A. S., Ouerfelli, O., Kirschner, M. W. and Rosen, M. K. (2004). Chemical inhibition of N-WASP by stabilization of a native autoinhibited conformation. *Nat. Struct. Mol. Biol.* **11**, 747-755.
Prehoda, K. E., Scott, J. A., Mullins, R. D. and Lim, W. A. (2000). Integration of multiple signals through cooperative regulation of the N-WASP-Arp2/3 complex. *Science* **290**, 801-806.
Proszynski, T. J., Gingras, J., Valdez, G., Krzewski, K. and Sanes, J. R. (2009). Podosomes are present in a postsynaptic apparatus and participate in its maturation. *Proc. Natl. Acad. Sci. USA* **106**, 18373-18378.
Quaranta, V., Walker, L. E., Pellegrino, M. A. and Ferrone, S. (1980). Purification of immunologically functional subsets of human Ia-like antigens on a monoclonal antibody (Q5/13) immunoadsorbent. *J. Immunol.* **125**, 1421-1425.
Rescigno, M., Urbano, M., Valzasina, B., Francolini, M., Rotta, G., Bonasio, R., Granucci, F., Kraehenbuhl, J. P. and Ricciardi-Castagnoli, P. (2001). Dendritic cells express tight junction proteins and penetrate gut epithelial monolayers to sample bacteria. *Nat. Immunol.* **2**, 361-367.
Sabeh, F., Ota, I., Holmbeck, K., Birkedal-Hansen, H., Soloway, P., Balbin, M., Lopez-Otin, C., Shapiro, S., Inada, M., Krane, S. et al. (2004). Tumor cell traffic through the extracellular matrix is controlled by the membrane-anchored collagenase MT1-MMP. *J. Cell Biol.* **167**, 769-781.
Sage, P. T., Varghese, L. M., Martinelli, R., Sciuto, T. E., Kamei, M., Dvorak, A. M., Springer, T. A., Sharpe, A. H. and Carman, C. V. (2012). Antigen recognition is facilitated by invadosome-like protrusions formed by memory/effector T cells. *J. Immunol.* **188**, 3686-3699.
Schachtner, H., Calaminus, S. D., Sinclair, A., Monypenny, J., Blundell, M. P., Leon, C., Holyoake, T. L., Thrasher, A. J., Michie, A. M., Vukovic, M. et al. (2013a). Megakaryocytes assemble podosomes that degrade matrix and protrude through basement membrane. *Blood* **121**, 2542-2552.
Schachtner, H., Calaminus, S. D., Thomas, S. G. and Machesky, L. M. (2013b). Podosomes in adhesion, migration, mechanosensing and matrix remodeling. *Cytoskeleton (Hoboken)* **70**, 572-589.
Schmidt, S., Nakchbandi, I., Ruppert, R., Kawelke, N., Hess, M. W., Pfaller, K., Jurdic, P., Fässler, R. and Moser, M. (2011). Kindlin-3-mediated signaling from multiple integrin classes is required for osteoclast-mediated bone resorption. *J. Cell Biol.* **192**, 883-897.
Schoumacher, M., Goldman, R. D., Louvard, D. and Vignjevic, D. M. (2010). Actin, microtubules, and vimentin intermediate filaments cooperate for elongation of invadopodia. *J. Cell Biol.* **189**, 541-556.
Shan, M., Gentile, M., Yeiser, J. R., Walland, A. C., Bornstein, V. U., Chen, K., He, B., Cassis, L., Bigas, A., Cols, M. et al. (2013). Mucus enhances gut homeostasis and oral tolerance by delivering immunoregulatory signals. *Science* **342**, 447-453.
Shimonkevitz, R., Kappler, J., Marrack, P. and Grey, H. (1983). Antigen recognition by H-2-restricted T cells. I. Cell-free antigen processing. *J. Exp. Med.* **158**, 303-316.
Strisciuglio, C., Duijvestein, M., Verhaar, A. P., Vos, A. C., van den Brink, G. R., Hommes, D. W. and Wildenberg, M. E. (2013). Impaired autophagy leads to abnormal dendritic cell-epithelial cell interactions. *J. Crohns Colitis* **7**, 534-541.
Takeda, K. and Akira, S. (2005). Toll-like receptors in innate immunity. *Int. Immunol.* **17**, 1-14.
Thornton, E. E., Looney, M. R., Bose, O., Sen, D., Sheppard, D., Locksley, R., Huang, X. and Krummel, M. F. (2012). Spatiotemporally separated antigen uptake by alveolar dendritic cells and airway presentation to T cells in the lung. *J. Exp. Med.* **209**, 1183-1199.
Tsujita, K., Kondo, A., Kurisu, S., Hasegawa, J., Itoh, T. and Takenawa, T. (2013). Antagonistic regulation of F-BAR protein assemblies controls actin polymerization during podosome formation. *J. Cell Sci.* **126**, 2267-2278.
Vallon-Eberhard, A., Landsman, L., Yogev, N., Verrier, B. and Jung, S. (2006). Transepithelial pathogen uptake into the small intestinal lamina propria. *J. Immunol.* **176**, 2465-2469.
van den Bogaart, G., Meyenberg, K., Risselada, H. J., Amin, H., Willig, K. I., Hubrich, B. E., Dier, M., Hell, S. W., Grubmüller, H., Diederichsen, U. et al. (2011). Membrane protein sequestering by ionic protein-lipid interactions. *Nature* **479**, 552-555.
van den Dries, K., van Helden, S. F., te Riet, J., Diez-Ahedo, R., Manzo, C., Oud, M. M., van Leeuwen, F. N., Brock, R., Garcia-Parajo, M. F., Cambi, A. et al. (2012). Geometry sensing by dendritic cells dictates spatial organization and PGE(2)-induced dissolution of podosomes. *Cell. Mol. Life Sci.* **69**, 1889-1901.
van den Dries, K., Meddens, M. B., de Keijzer, S., Shekhar, S., Subramaniam, V., Figdor, C. G. and Cambi, A. (2013a). Interplay between myosin IIA-mediated contractility and actin network integrity orchestrates podosome composition and oscillations. *Nat. Commun.* **4**, 1412.
van den Dries, K., Schwartz, S. L., Byars, J., Meddens, M. B., Bolomini-Vittori, M., Lidke, D. S., Figdor, C. G., Lidke, K. A. and Cambi, A. (2013b). Dual-color

superresolution microscopy reveals nanoscale organization of mechanosensory podosomes. *Mol. Biol. Cell* **24**, 2112-2123.

van Helden, S. F., Krooshoop, D. J., Broers, K. C., Raymakers, R. A., Figdor, C. G. and van Leeuwen, F. N. (2006). A critical role for prostaglandin E2 in podosome dissolution and induction of high-speed migration during dendritic cell maturation. *J. Immunol.* **177**, 1567-1574.

Vestweber, D. (2012). Novel insights into leukocyte extravasation. *Curr. Opin. Hematol.* **19**, 212-217.

von Kleist, L., Stahlschmidt, W., Bulut, H., Gromova, K., Puchkov, D., Robertson, M. J., MacGregor, K. A., Tomilin, N., Pechstein, A., Chau, N. et al. (2011). Role of the clathrin terminal domain in regulating coated pit dynamics revealed by small molecule inhibition. *Cell* **146**, 471-484.

West, M. A., Prescott, A. R., Chan, K. M., Zhou, Z., Rose-John, S., Scheller, J. and Watts, C. (2008). TLR ligand-induced podosome disassembly in dendritic cells is ADAM17 dependent. *J. Cell Biol.* **182**, 993-1005.

Wiesner, C., Faix, J., Himmel, M., Bentzien, F. and Linder, S. (2010). KIF5B and KIF3A/KIF3B kinesins drive MT1-MMP surface exposure, CD44 shedding, and extracellular matrix degradation in primary macrophages. *Blood* **116**, 1559-1569.

Wolf, K. and Friedl, P. (2009). Mapping proteolytic cancer cell-extracellular matrix interfaces. *Clin. Exp. Metastasis* **26**, 289-298.

Wolf, K., Te Lindert, M., Krause, M., Alexander, S., Te Riet, J., Willis, A. L., Hoffman, R. M., Figdor, C. G., Weiss, S. J. and Friedl, P. (2013). Physical limits of cell migration: control by ECM space and nuclear deformation and tuning by proteolysis and traction force. *J. Cell Biol.* **201**, 1069-1084.

Yamaguchi, H., Yoshida, S., Muroi, E., Kawamura, M., Kouchi, Z., Nakamura, Y., Sakai, R. and Fukami, K. (2010). Phosphatidylinositol 4,5-bisphosphate and PIP5-kinase Ialpha are required for invadopodia formation in human breast cancer cells. *Cancer Sci.* **101**, 1632-1638.

Zicha, D., Allen, W. E., Brickell, P. M., Kinnon, C., Dunn, G. A., Jones, G. E. and Thrasher, A. J. (1998). Chemotaxis of macrophages is abolished in the Wiskott-Aldrich syndrome. *Br. J. Haematol.* **101**, 659-665.